Proceedings of the 17th World Congress
The International Federation of Automatic Control
Seoul, Korea, July 6-11, 2008

Compensation of sub-harmonic vibrations during engine idle by variable fuel injection control

Andreas Walter *, **Mustafa Murt** *, **Uwe Kiencke** *
Stephen Jones **, **Thomas Winkler** **

* *Institute of Industrial Information Technology, Universität Karlsruhe (TH), Germany*
** *LuK GmbH & Co. oHG, Germany*

Abstract: Today, in many passenger cars and light trucks, the conventional driveline is extended by a dual mass flywheel (DMF). The DMF reduces driveline oscillations by mechanically decoupling the transmission from the periodic combustion events that excite the engine crankshaft. Existing engine control systems are designed for conventional single mass flywheel (SMF) systems. In the future, to facilitate the optimal control of engines equipped with advanced DMF systems, such conventional control systems may require adaptation, modification or even replacement. The basic task of idle speed control systems is to maintain a defined setpoint of rotational engine speed independent from engine operating conditions (e.g. load disturbances). Due to the torque reactions of the DMF, control systems designed for engines with SMF can be disturbed, leading to unstable engine idle (e.g. sub-harmonic vibrations, oscillations following load rejection, etc.) In this approach, an optimised solution for idle speed control regarding conventional combustion engines equipped with DMF is introduced. The enhanced control system is based on conventional PID-control strategies with improved fuel injection scheduling. Using incremental (i.e. tooth-to-tooth) engine speed, critical dead times, which can lead to limit cycles in non-linear closed-loop control circuits, are minimised. Limit cycles, which are distinguishable as sub-harmonic vibrations at the same frequency, are effectively reduced by improving load rejection at idle. The implementation of these solutions in current engine management systems requires no additional sensors or other hardware.

Keywords: idle speed control; idle speed controller (ISC); engine speed filter; PID controller; shaped P- & I-gains; idle speed; sub-harmonic vibrations; decoupled idle speed control (DISC), injection control; injection duration; proportional; integral; idle speed governor; load rejection; DMF; TMF; TMFW.

1. INTRODUCTION

Due to the periodic combustion processes in conventional automotive vehicles the crankshaft inertia is excited by an oscillating engine torque. These oscillations induce noise and degrade driveability. Various mechanical solutions e.g. the dual mass flywheel (DMF) have been developed to isolate and reduce these oscillations (Figure 1). A simple DMF (Figure 2) basically consists of two separate flywheels connected by long travel arc-springs for damping the engine speed oscillations. The DMF is located between the engine and the clutch and replaces the conventional single mass flywheel (SMF). Beside the advantages of the DMF (noise prevention, reduced fuel consumption, lower crankshaft and transmission stresses, etc.) the non-linear behaviour of the DMF also increases the system complexity. Due to its capability of energy storage, the DMF generates a torque reaction on both the crankshaft and driveline. Existing engine control algorithms are generally designed for use with conventional SMF systems and are based on the crankshaft rotational speed. With the assumption that the load torque, reacting on the crankshaft via the clutch, is approximately constant within one combustion cycle, disturbances of the engine torque (e.g. imbalanced cylinders, misfiring, etc.) can be successfully detected and regulated. For idle speed control, a SMF with no reacting driveline torque (equivalent to an open clutch) has often been presumed. The fast changing DMF load torque reacting on the crankshaft, means that these assumptions are not always achieved in practice. Increasing cylinder to cylinder torque differences with ever higher fuel injection pressures have further exacerbated this problem. These factors can lead to problems when conventional

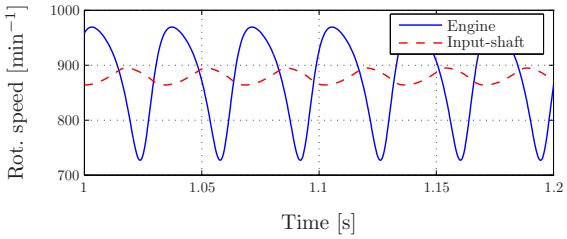

Fig. 1. Engine and input-shaft speed for vehicles using dual mass flywheels

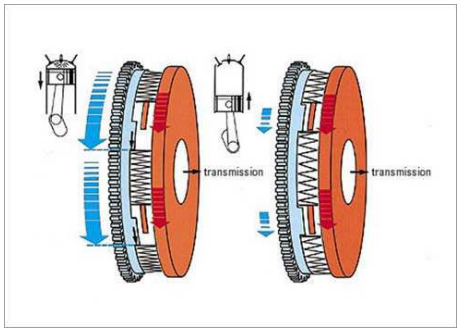

Fig. 2. Basic principle of the Dual Mass Flywheel

engine management system control algorithms are used on vehicles equipped with dual mass flywheels. In the future, to facilitate the optimal control of engines equipped with advanced DMF systems, such conventional control systems may require adaptation, modification or even replacement.

In this paper, an advanced solution for idle speed control (ISC), that takes the system behaviour of the DMF into account is introduced. An advanced ISC system has to fulfil various important demands regarding idle stability, including the elimination, or at least a reduction, of any tendency towards sub-harmonic vibrations, as well as providing robust external load rejection.

2. CONVENTIONAL PID IDLE SPEED CONTROL

Many conventional combustion engine idle speed controllers (ISC) are based on standard PID-control theory [Kiencke and Nielsen (2005)]. A conventional PI-ISC is shown in figure 3.

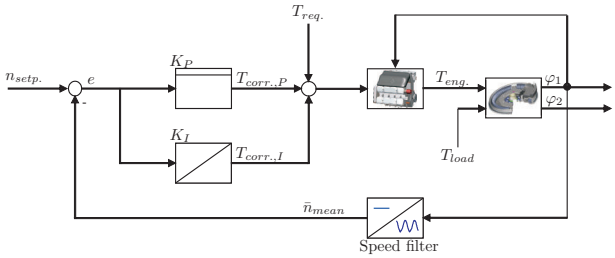

Fig. 3. Principal structure of a conventional PI-ISC

Here, the differential D part of the controller has been set to zero. The mean primary flywheel speed (i.e. engine speed) is determined by the engine speed filter. Speed filters provide mean engine speeds, that are valid for a specified segment of crankshaft evolution (e.g. $\Delta\varphi_{sf} = 180°$). Due to the averaging process, the static engine speed determined is valid for the next crankshaft segment $\Delta\varphi_{sf}$. Thus, a large angular speed filter segment $\Delta\varphi_{sf}$ effects a long delay in the updating of the mean engine speed in the engine ECU. After filtering the engine speed, the mean value $\bar{n}_{mean}$ is subtracted from the required idle speed setpoint $n_{setp.}$. The resulting error signal e is passed to the PI controller, that determines the ISC correction torque $T_{ISC,i}$. The combustion engine itself excites the dual mass flywheel and completes the circuit of the non-linear control system. Usually, the PI-ISC is integrated within the engine Electronic Control Unit (ECU), which calculates the required fuel injection quantity for each cylinder individually. The fuel injection calculation is often based on a torque balance, where each sub-system for engine control contributes its individual correction torque.

$$T_{engine,total} = T_{req.} + \sum_i T_{corr.,i} \quad (1)$$

$T_{req.}$ is the engine torque demanded by the driver. All correction torques $T_{corr.,i}$ have to be calculated and relayed to the injection control unit a specified minimum angular distance [1] $\Delta\varphi_{i,inj.}$ before the start of fuel injection is scheduled to begin (Figure 4). The angular window for collecting the individual engine correction torques starts at $\varphi_{i,acq.}$

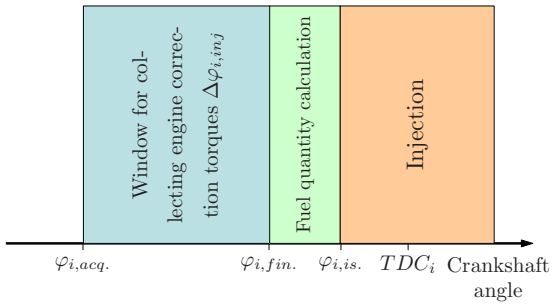

Fig. 4. Fuel injection calculation sequence

Once $\Delta\varphi_{i,inj.}$ has elapsed, the control intervention $T_{corr.,i}$ has to be shifted to the injection for the next cylinder $i+1$. The injection starts at $\varphi_{i,is.}$. In many cases, the magnitude of both the P- and I-gain of the ISC also depend on the actual error signal e, so called P- and I-gains shaping (i.e. gain scheduling) (Figure 5).

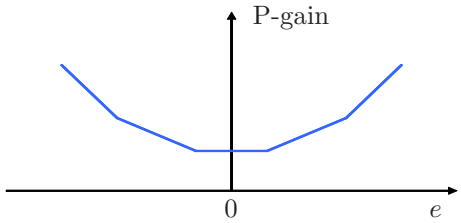

Fig. 5. ISC P-gain scheduling

This provides increased versatility for application specific ISC tuning during the engine calibration process. PI-controllers with very low P-gains offer reduced sub-harmonic vibrations (see section 3) at idle, but have the disadvantage of relatively poor load rejection. High P-gains provide better load rejection but tend to exacerbate sub-harmonic vibrations. Therefore, a compromise between these two important but sometimes conflicting control goals has to be found. In some cases the capabilities of gain scheduling are not extensive enough to fulfil all of the demands made on the ISC system (i.e. excellent idle speed stability with zero or minimal sub-harmonic vibrations, combined with excellent load rejection). Re-design of mechanical components (e.g. DMF) and/or improved engine control algorithms may also be required. During the re-design process, extensive simulation as well as calibration efforts may be necessary, increasing the product development time and cost.

[1] angular rotation of crankshaft

3. SUB-HARMONIC VIBRATIONS

In the non-linear internal combustion engine ISC circuit sub-harmonic vibrations can occur. Here, *sub-harmonic* means, that the frequency of this vibration is an integer fraction of the engine's firing frequency. A four-cylinder four-stroke engine exhibits second order firing, which means, that two combustion events occur per crankshaft revolution. Commonly observable sub-harmonic vibrations for four-cylinder engines with dual mass flywheel have 0.5th, 0.66th and first orders (Figure 6).

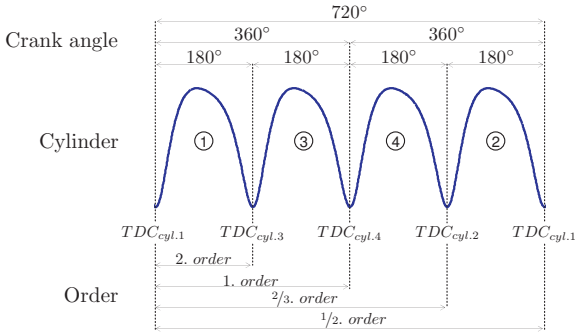

Fig. 6. Order of sub-harmonic vibrations on a 4-cylinder 4-stroke engine

Sub-harmonic vibrations are typically excited by sudden changes of engine or driveline load. Load changes at the crankshaft and the rigidly connected primary DMF flywheel can be induced by the switching of high electrical loads or air conditioning. Driveline load changes acting on the secondary flywheel of the DMF can be induced by engaging and disengaging the clutch pedal (Figure 7).

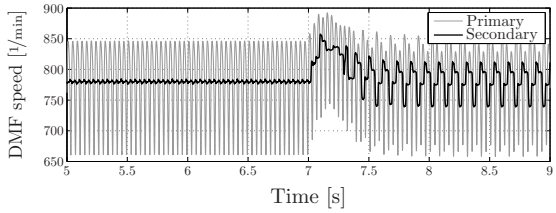

Fig. 7. Sub-harmonic vibrations excited by primary flywheel side load change

At $t = 7s$, a primary load acting on the crankshaft (e.g. air conditioning) of $T_{load,prim.} = 15Nm$ has been switched off. The conventional PI-ISC described in figure 3 shows adequate load rejection behaviour by quickly reducing the mean engine speed $\bar{n}_{mean}$ to the defined set-point $n_{setp.}$. However, after reaching the nominal engine idle speed, the primary, as well as the secondary flywheels of the DMF show sub-harmonic oscillations. Sub-harmonic vibrations (SHV) can also be excited by positive load steps. Even a short torque impulse (e.g. that caused by short clutch pedal engagement) acting on primary or secondary flywheel can lead to SHVs.

One might think, that idle SHVs are mainly due to the non-linear behaviour of the DMF. However, idle SHVs are also observable in vehicles fitted with conventional single mass flywheels; even on those with perfectly balanced engine cylinders. An important question is therefore, which parts of the highly non-linear ISC circuit provoke sub-harmonic vibrations. In order to answer this question, the so-called *Harmonic Balance Method* [Föllinger (1987)] has been used to analyse the non-linear engine ISC circuit.

4. HARMONIC BALANCE

The elements of the closed-loop control circuit are separated into two types: linear and non-linear.

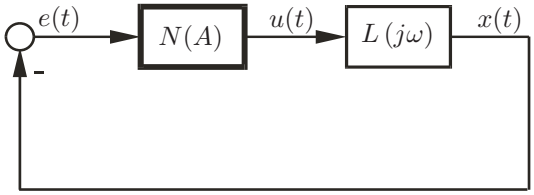

Fig. 8. Non-linear control circuit with separated elements

$L(j\omega)$ is the transfer function of the linear system elements, whereas $N(A)$ is the describing function of the non-linear (Figure8). The basic idea of the Harmonic Balance method is that the closed loop system performs limit cycles. In this case, e, u, and $x = -e$ are periodic functions. For periodic functions, the Fourier expansion is mathematically tractable.

$$u(t) = b_0 + \sum_{\nu=1}^{\infty} \left[a_\nu \cdot \sin(\nu\omega_p t) + b_\nu \cdot \cos(\nu\omega_p t)\right] = b_0 + \sum_{\nu=1}^{\infty} C_\nu \cdot \sin(\nu\omega_p t + \varphi_\nu) \quad (2)$$

During steady state limit cycles, each sinusoidal signal $u(t)$ generates also a sinusoidal signal [2] $x(t)$ at the same frequency.

$$x(t) = \sum_{\nu=1}^{\infty} |L(j\nu\omega_p)| \cdot C_\nu \sin\left[\nu\omega_p t + \varphi_\nu + \angle L(j\nu\omega_p)\right] \quad (3)$$

Here, the non-linear describing function $N(A)$ is processing the signal by obtaining the frequency.

$$e \rightarrow \tilde{e} = Ae^{j\omega t} \quad (4)$$

$$u \rightarrow u_1 = C_1 e^{j(\omega t + \varphi_1)} \quad (5)$$

A is the amplitude of the error signal e. Assuming a strong low-pass linear transfer function characteristic, only the first Fourier coefficient C_1 is taken into account. Therefore the non-linear describing function can be written as:

$$N(A) = \frac{\tilde{u}_1}{\tilde{e}} = \frac{C_1}{A} e^{j\varphi_1} = \frac{C_1 \cos\varphi_1}{A} + j\frac{C_1 \sin\varphi_1}{A} = R(A) + jI(A) \quad (6)$$

where $R(A)$ and $I(A)$ can be determined by calculating the Fourier coefficients of the known non-linear characteristic curve $F(e, \dot{e})$.

$$R(A) = \frac{1}{\pi A} \int_0^{2\pi} F(A\sin v, \omega A \cos v) \sin v dv \quad (7)$$

$$I(A) = \frac{1}{\pi A} \int_0^{2\pi} F(A\sin v, \omega A \cos v) \cos v dv \quad (8)$$

After determining $N(A)$, a condition for steady state limit cycles, the so-called characteristic equation of the harmonic balance can be established:

$$[L(j\omega)N(A) + 1]\, e = 0 \quad (9)$$

[2] due to the symmetry of the non-linear characteristic curve, b_0 is zero

For steady state limit cycles, the linear transfer function $L(j\omega)$ has to be equal to the negative reciprocal value of the describing function $N(A)$.

$$L(j\omega) = -\frac{1}{N(A)} =: N_J(A) \tag{10}$$

The left hand of equation (10) describes the linear Nyquist Plot (NP) $L(j\omega)$, whereas $N_J(A)$ is the non-linear NP. By plotting both, linear as well as non-linear NP in one diagram, the intersection of both curves reveals limit cycles in the non-linear control system [Föllinger (1987)]. Additionally, a stability criterion analogous to the *Nyquist Criterion* [Levine (1996)] can be derived. An intersection of NPs indicates a stable limit cycle, if the non-linear NP crosses the linear NP from right to left at rising amplitude A.

Sub-harmonic vibrations in the non-linear ISC circuit can be interpreted as limit cycles. Therefore the Harmonic Balance method allows the analysis of SHVs at idle.

5. ANALYTIC DESCRIPTION OF ISC SUB-COMPONENTS

According to [Walter et al. (2006)], conventional internal combustion engines represent extremely complex and non-linear thermo-mechanical systems. In the past, many approaches have been used to construct engine models, which accurately approximate the actual engine state. One established conclusion is, that the type of engine model employed has to be selected according its intended use. Otherwise it would be too complex to fulfil restrictions due to computational efficiency. Usually, for ISC development, knowledge of the static (i.e. mean value) engine torque is sufficient. A commonly used method for modelling the static engine torque is described by Kiencke and Nielsen (2005). As figure (9) illustrates, the stationary engine behaviour can be described by a first-order delay combined with a dead-time element.

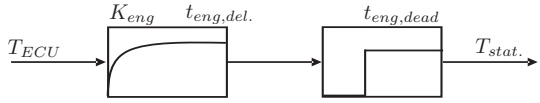

Fig. 9. Simple model for static engine torque

The transfer function of this model is:

$$\begin{aligned} G_{engine}(s) &= G_{delay}(s) \cdot G_{dead}(s) \\ &= \frac{1}{1 + t_{eng,del.} \cdot s} \cdot e^{-t_{eng,dead} \cdot s} \end{aligned} \tag{11}$$

Note, the transfer function $G_{engine}(s)$ include linear $G_{delay}(s)$ as well as non-linear $G_{dead}(s)$ proportions. Due to the multiplicative combination, these proportions may be interchanged. The DMF is directly connected to the crankshaft of the combustion engine. The DMF characteristic curves demonstrate its highly non-linear behaviour (Figure 10).

At idle speed, the DMF can approximately be described by an equivalent SMF with backlash (Figure 11).

Here, J is the total inertia of the DMF. Based on the second Newtonian axiom for rotating inertias, the transfer function of an equivalent SMF can be written as:

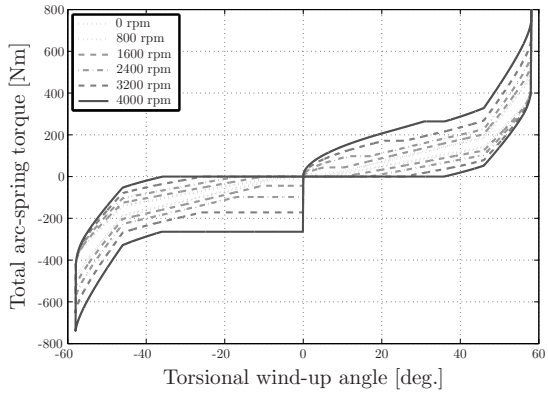

Fig. 10. Non-linear characteristics of DMF arc-springs

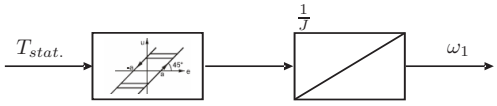

Fig. 11. Non-linear characteristics of DMF arc-springs

$$G_{SMF}(s) = \frac{\Omega_1(s)}{T(s)} = \frac{1}{s} \cdot \frac{1}{J} \tag{12}$$

$G_{SMF}(s = j\omega)$ represents the linear proportion of the simplified DMF sub-system. The non-linear proportion is described by a backlash. According to Föllinger (1987), the describing function of a backlash is:

$$\begin{aligned} N(\alpha) = \frac{1}{2} + \frac{1}{\pi}\left[\arcsin\alpha + \alpha\sqrt{1-\alpha^2}\right] \\ - j\frac{1}{\pi}\left(1-\alpha^2\right) \end{aligned} \tag{13}$$

with

$$\alpha = 1 - \frac{2\varphi_s}{A}; \qquad -1 < \alpha < 1 \tag{14}$$

As shown in figure 3, the mean engine speed is determined over a defined angular crankshaft segment $\Delta\varphi_{sf}$. Generally, real-time engine speed measurement is performed using an inductive sensor and toothed rim or sensor ring gear (Figure 12).

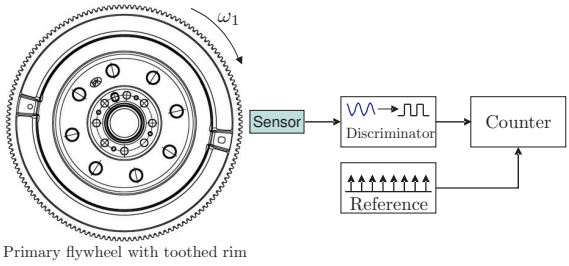

Fig. 12. Engine speed measurement system

Therefore, the speed filter contributes an additional dead time $t_{sf,dead}$ to the ISC feedback loop.

$$t_{sf,dead} = \frac{\overline{\omega}_1}{\Delta\varphi_{sf}} \tag{15}$$

The PI-ISC itself contributes two linear parallel components. However, due to the fact, that the proportional P-gain part of the controller is mainly responsible for the occurrence of sub-harmonic vibrations, the I-gain is omitted and only a simple P-gain controller is used. It can be shown that with regard to SHVs, variations of the integral I-gain have significantly less influence than variations the

P-gain. This is partly due to the fact, that the integral part of the ISC is generally relatively small compared to the proportional part. The basic task of the I controller is to ensure ISC set-point achievement i.e. eliminate the steady state error. Therefore, the ISC speed filter and controller can be simply described as a proportional gain combined with a dead-time element (Figure 13).

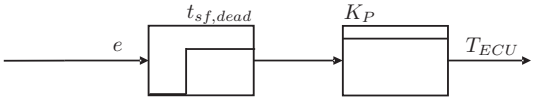

Fig. 13. Simplified ISC structure with speed filter

The transfer function of the ISC with speed filter is given by:

$$G_{ISC}(s) = K_P \cdot e^{-t_{eng,dead}s} \tag{16}$$

Assembling these simplified sub-system models together, reveals the following non-linear ISC system structure (Figure 14).

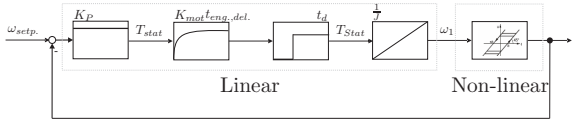

Fig. 14. Structure of simplified ISC system

The components of the total closed-loop system can be divided into linear and non-linear parts. Due to the fact, that the Nyquist plots of dead time elements are well known, the dead time $t_d = t_{eng.,dead} + t_{sf,dead}$ can be allocated to the linear part. Therefore, the non-linear part of the total system contains solely the backlash of the DMF. The corresponding non-linear Nyquist plot $N_J(A)$ based on (13) is shown in figure 15.

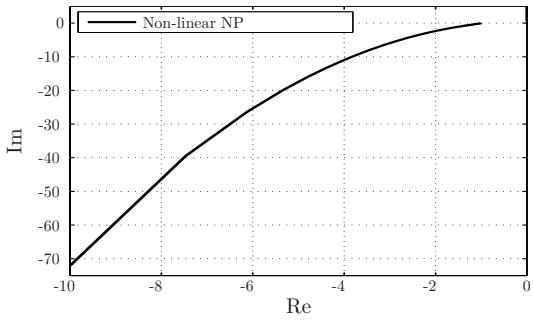

Fig. 15. Nyquist plot (NP) of non-linear ISC part

For increasing amplitudes A, $N_J(A)$ tends to infinity. The shape of the curve does not vary by changing either A or α.

The transfer function $L(s)$ of the total ISC system is created by combining all of the various linear sub-elements previously introduced.

$$\begin{aligned} L(s) &= G_{ISC}(s) \cdot G_{engine}(s) \cdot G_{SMF}(s) \\ &= K_P \cdot \frac{K_{eng}}{1 + t_{eng,del.} \cdot s} e^{-t_d s} \cdot \frac{1}{s \cdot J} \end{aligned} \tag{17}$$

The NP of the $L(s)$ is:

$$L(j\omega) = \frac{K}{j\omega(1 + j\omega t_{e,d})} \cdot e^{-j\omega t_d} \tag{18}$$

with

$$K = \frac{K_P \cdot K_{eng}}{J} \tag{19}$$

Figure 16 shows some examples to help visualise the shape of the NP with different parameter values.

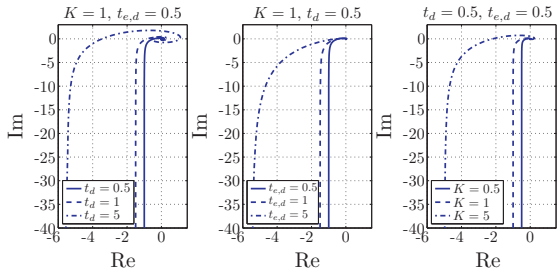

Fig. 16. Nyquist plots (NP) of the linear ISC part

Compared to the non-linear NP, the linear NP changes its shape during parameter variation of K, $t_{e,d}$ and t_d. This means, that the parameters of the linear ISC system components can be adjusted to prevent intersection of linear and non-linear NP, eliminating or minimising sub-harmonic vibrations (Figure 17). Note, not all ISC parameters can arbitrarily be changed without limit. In many cases, there are other restrictions on the parameters of the ISC to ensure proper functionality for all operating points (e.g. a high P-gain may be required to ensure adequate load rejection). Due to the construction of the engine and the structure of conventional ISC speed filters, some parameters, especially dead time elements cannot easily be reduced.

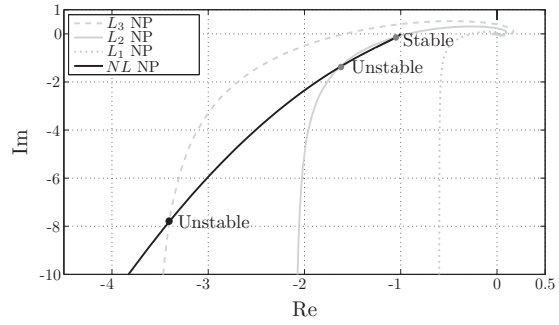

Fig. 17. Nyquist Plot used to solve the characteristic equation of harmonic balance

The NP of various different linear transfer functions (Figure 17) allows a classification into three basic categories. In the first case, no intersection of linear and non-linear NP exists. Thus, no limit cycles occur in the ISC control system and no SHVs are observed. As shown in figure 16, Nyquist Plots similar to L_1 NP can be realised by small P-gains or short dead-times. In the second case (L_2 NP), there are two intersection in the NP. For this configuration a stable as well as an unstable limit cycle can occur at different operating points. Whereas the stable limit cycle would lead to sub-harmonic vibrations, the unstable indicates a completely unstable system. By ensuring that the system will never reach a operating point of a unstable limit cycle, L_2 NP would lead to a sub-optimal solution with SHVs (commonly observable in reality). The third category (L_3 NP) shows only one unstable intersection. Therefore, this ISC parameterisation leads to unstable system behaviour. This case occurs for high P gains or long dead times.

It is important to remember, that the sub-components of the ISC control circuit model used include various simplifications. Therefore to validate the results of this Harmonic Balance ISC analysis, it is necessary to run both simulated and actual test cycles of the proposed ISC system to ensure its reliable functionality under a range of real world conditions. However, analysis based on the Harmonic Balance method allows a deeper understanding of how the system parameters can be systematically tuned and therefore supports the more rapid development of better and more robust ISC systems.

6. IMPROVED ISC CONCEPT FOR REDUCING SHVS

There are two main ways of improving conventional ISC systems with respect to reducing the risk of sub-harmonic vibrations. Firstly, the proportional part K of the closed-loop can be reduced. According to equation (19) K can be decreased by higher primary flywheel inertias J and low P-gains K_P at ISC. Generally, the engine gain $K_{eng.}$ cannot be reduced without engine redesign. Higher flywheel inertias J increase the engine weight and fuel consumption, degrade performance feel and are difficult to package. One option is to significantly reduce the proportional P-gain of the ISC. However, this solution stands contrary to good load rejection. A compromise between these conflicting objectives can sometimes be found by intelligently calibrating ISC gain schedules as a function of error signal, the possibility for which is already available in many engine ECUs. A second possibility of reducing the risk of SHVs is to minimise the system dead-time. The total dead-time of the engine and control system is due to combustion engine processes, the engine ECU speed filter, the ISC and injection scheduling processes.

$$t_d = t_{eng,dead} + t_{sf,dead} \tag{20}$$

By changing the speed filter dead time $t_{sf,dead}$, the probability of occurrence of limit cycles and thus SHVs can be significantly reduced. As described in section 2, the speed filter dead time exists due to the fact, that the mean engine speed is calculated over a defined angular crankshaft window or segment $\Delta\varphi_{sf}$. By reducing this window for mean value acquisition, the dead time of the speed filter can be significantly reduced. The strongest reduction of dead time is attained with the use of an incremental i.e. tooth-to-tooth engine speed $\overline{n}_{t2t}$, instead of a filtered mean engine speed. In order to realise this, the proportional controller has been separated from other ISC and engine ECU software modules and is supported by tooth-to-tooth engine speed which can be applied just before or perhaps even during the scheduled fuel injection event (Figure 18).

The integral term as well as the other engine control systems are maintained using a conventional mean engine speed signal $\bar{n}_{\Delta\varphi_{i,ec}}$, calculated over a defined angular segment $\Delta\varphi_{i,ec}$.

For validation, this modified control system is compared to the conventional PI-ISC system shown in figure 3. The results are shown in figure 19 and figure 20. For validation, a dynamic 2.0 litre 4-cylinder diesel engine model [Walter et al. (2006)] and a highly realistic DMF model [Reik et al. (1998)], where each coil of the arc-springs is modeled

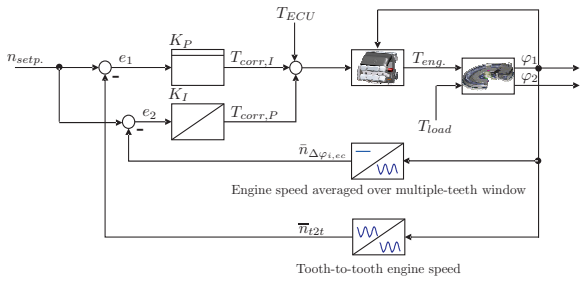

Fig. 18. ISC with proportional term based on tooth-to-tooth engine speed

separately, were used. Both of these sub-system models were themselves developed, calibrated and validated using measured test data.

Figure 19 shows simulation results for a conventional PI-ISC system according to section 2. At $t = 4s$ a primary side load torque is switched on. The engine speed decreases slightly but soon recovers to the idle speed set-point $n_{setp.}$. During the high load phase, weak sub-harmonic vibrations occur. After the load is switched off, the engine speed as well as the secondary flywheel speed include strong sub-harmonic vibrations. These oscillations remain until after the load changes. If the load is constant, the SHVs do not decay (i.e. a stable limit cycle exists). After $t = 7s$, a short pulse acting on secondary DMF side is introduced. Such a load profile can be generated with the clutch pedal. After the impulse, the engine speed returns to its original condition before any load changes were applied.

Figure 20 shows the modified PI-ISC system which uses tooth-to-tooth engine speed signal as the input to the proportional controller. Here, the same load torque profiles as used in figure 19 were applied. Sub-harmonic vibrations, in both the primary and secondary side speeds of the DMF, are significantly reduced compared to the conventional PI-ISC system. Some SHVs appear during a positive step of the secondary side load, but decay away within a few seconds. Note, these results have been validated for a range of engine-DMF-speed filter configurations.

Additional results from further parameter variation simulations, are shown in figure 21. Here, some of the manufacturing and lifetime tolerances of the DMF are varied. *SDF* is the static displacement friction for the arc-springs in the channel. $\Delta\varphi_{F,AS}$ is the free angle between the DMF flange and arc-spring. Each cell of these 'traffic light' style diagrams represents a simulated idle test cycle with fixed DMF parameters. Sub-harmonic vibrations with amplitudes higher than $5rpm$ are shown in red. In figure 21 SHVs of $0.5th$ order were detected. The diagram for the modified ISC system shows considerably less red cells than the conventional ISC. Similar results were realised for SHVs of the 0.66 and first orders.

The main disadvantage of supplying the proportional controller with the tooth-to-tooth engine speed signal as an input, is that stochastic signal noise disturbances may have a greater effect when compared to a conventional P-controller utilising a mean engine speed input signal. The adoption of tooth-to-tooth engine speed for ISC, may require more accurate sensors, sensor ring gears and / or additional algorithms [Kiencke and Eger (2004)] for speed

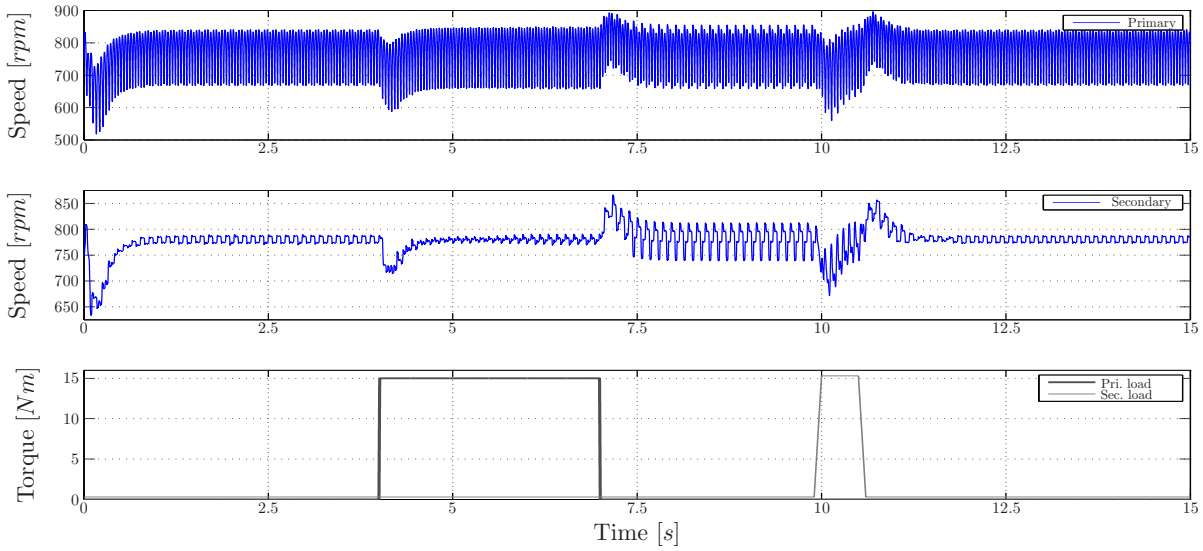

Fig. 19. Validation of conventional PI-ISC

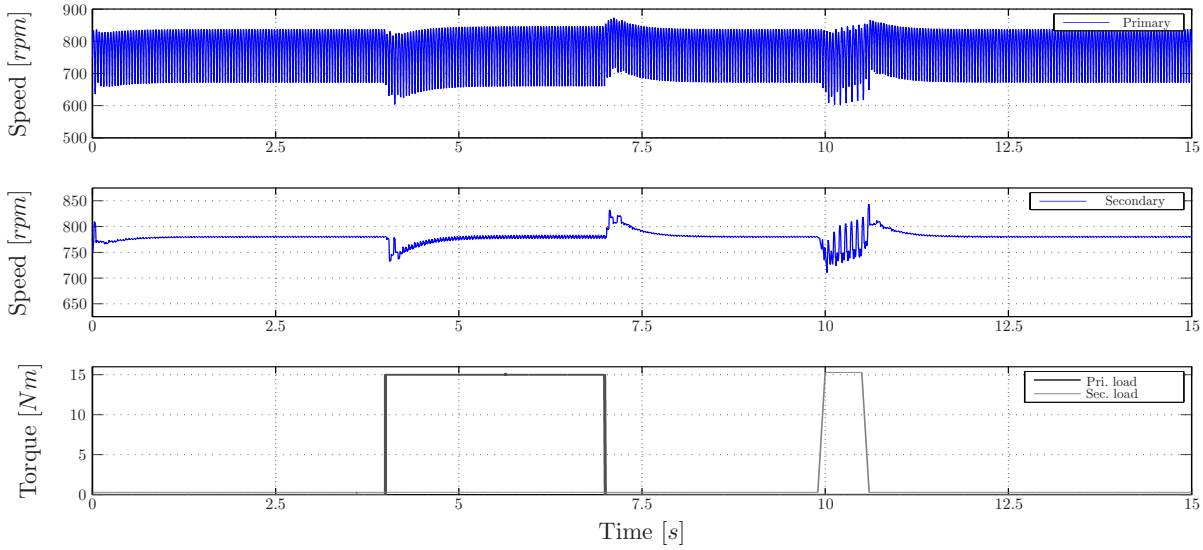

Fig. 20. Validation of modified PI-ISC using tooth-to-tooth engine speed

signal processing to provide a sufficiently reliable information. Mean speed values over two or more teeth increase the systems robustness regarding sensor noise, but on the other hand increase the dead time in the ISC system. Another solution could be the usage of enhanced control algorithms [Åström and Hägglund (2005)], that are taken the dead time into account and fully replace conventional PID-ISC. The actual dead time of the engine speed filter $t_{sf,dead}$ is also influenced by the final acceptance angle $\varphi_{i,fin.}$ of injection control (IC) in the ECU. As indicated in figure 4, sending a correction torque to the IC for the next injection, is only possible within a defined angular window $\Delta\varphi_{i,inj} = \varphi_{i,fin.} - \varphi_{i,acq.}$ for conventional IC systems. After $\varphi_{i,fin.}$, no correction torque for the upcoming injection can be transmitted to the IC. However, by structurally decoupling the proportional part of the conventional PI-ISC, the dead time can be significantly further reduced.

Due to the fact, that the proportional ISC part contributes a static engine torque correction $T_{ISC,P,corr.} = K_P \cdot (n_{setp.} - \overline{n}_{T2T})$ based on two simple numerical operations, the addition of this correction torque, which corresponds to a defined fuel quantity per stroke, can be executed as close as possible to the actual start of fuel injection $\varphi_{i,is.}$. By decoupling the correction torque $\Delta T_{ISC,P,corr.}$ and executing the basic ISC-P control in the conventional injection calculation sequence, only a small change (i.e. final correction) of the current ISC-P control is performed close to the start of injection. In the worst case this final correction of ISC-P may even fail, due for example to non-reliable speed sensor information, without any risk to the basic function of ISC. Using a small proportional ISC correction torque $\Delta T_{ISC,P,corr.}$, fast acting fuel injectors (e.g. piezo injectors) allow even an adaptation of the injection discharge rate. Hence, the correction torque $\Delta T_{ISC,P,corr.}$ can be applied close to the end of injection and thus include precious up to date engine speed information. Consequently, this method provides a sophisticated ISC solution which delivers a high degree of engine idle stability and smoothness as well as providing excellent load rejection.

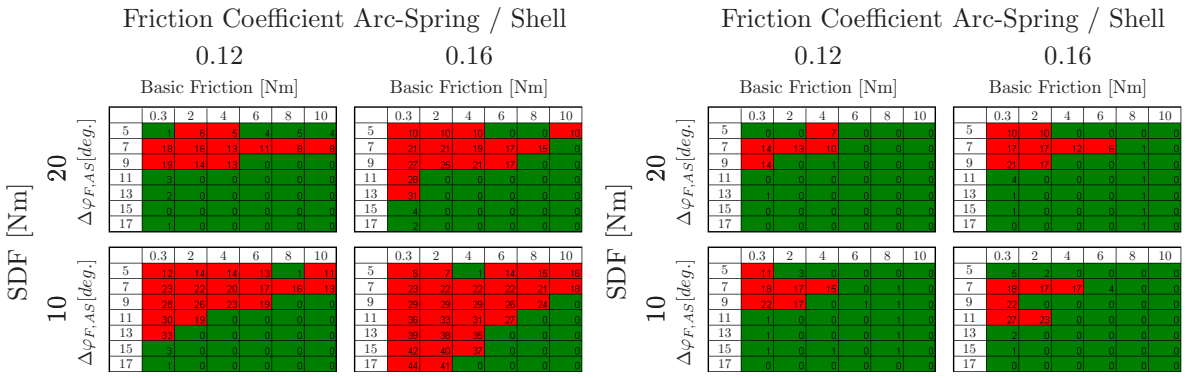

(a) conventional PI-controller (b) T2T PI-controller

Fig. 21. Parameter variation for ISC validation: 0.5th order SHVs

One outstanding advantage of the introduced modified PI-ISC system is, that no additional hardware is required for its implementation. The input variable for the ISC-P described is the existing tooth-to-tooth engine crankshaft signal. Taking into account, that some engine ECUs already make use of tooth-to-tooth speed or time information, an implementation of the improved ISC system described is technically possible. However, control intervention close to the start of fuel injection, or even by changing the injection discharge rate with a small ISC correction $\Delta T_{ISC,P,corr.}$, will require some software modifications to current engine ECUs.

7. CONCLUSION AND OUTLOOK

In this approach, the limitations of conventional PI-idle speed controllers, especially for vehicles fitted with DMF, have been introduced. For conventional systems, a compromise between reducing sub-harmonic vibrations and adequate load rejection has to be found. By using the so-called Harmonic Balance method, this problem has been carefully inspected. SHVs are limit cycles in non-linear ISC control systems. These limit-cycles can be significantly reduced with lower P-gains and shorter system dead times. Due to the fact, that low P-gains limit ISC load rejection, a method, reducing the dead time in the complete engine control system has been developed. Here, the proportional ISC part is decoupled from other engine control systems. The input variable for the P-controller is the incremental or tooth-to-tooth engine speed. This combined with separate software sequences for fuel injection control leads to a robust and efficient concept for future ISC systems, that minimises SHVs and offers improved load rejection. The system has been tested and verified using various parametric simulations.

Due to its relatively easy integration within existing control systems, this improved ISC system could be tested and validated by simply adapting current engine control software. Such tests would indicate whether additional signal processing algorithms for sensor data conditioning and / or improved speed sensor concepts are required to provide a reliable tooth-to-tooth engine speed signal for idle speed control.

REFERENCES

K. J. Åström and T. Hägglund. *Advanced PID Control*. ISA, 2005.

O. Föllinger. *Nichtlineare Regelungen, vol.1*. Oldenburg Verlag, München and Wien, 1987.

U. Kiencke and R. Eger. *Messtechnik*. Springer-Verlag Berlin Heidelverg, 2004.

U. Kiencke and L. Nielsen. *Automotive Control Systems, 2. Edition*. Springer-Verlag, Berlin Heidelberg, 2005.

W. S. Levine. *The control handbook*. Boca Raton : CRC Press, 1996. ISBN 0-8493-8570-9.

W. Reik, R. Seebacher, and A. Kooy. *Dual Mass Flywheel*. 6. LuK Kolloquium, 1998.

A. Walter, B. Merz, U. Kiencke, and S. Jones. *Comparison & Development of Combustion Engine Models for Driveline Simulation*. SAE Word Congress 2006, Detroit, USA, 2006.